the height between the model-release point and the water surface.

The accelerations were measured by strain-gage type accelerometers, and the records were traced on an oscilloscope and photographed. The two accelerometers used were a ± 100 g Kyowa accelerometer with a natural frequency of 2000 cps and a ± 200 g accelerometer with a natural frequency of 3000 cps. Both were damped to 65% of critical damping. A Kyowa amplifier was used which had a carrier frequency of 20,000 cps.

Experimental Results

The tests were repeated 3–5 times each, and the measured values of v_0, n_m, and τ_m scatter within 5% of the mean value. Therefore the mean values are used for the comparison with the analytical results.

The experimental results and the comparison with the theoretical values for the spherical models are presented in Table 2 and Fig. 2. An acceleration-time history curve is shown in Fig. 3a. This photographic record shows the oscillatory characteristics of the acceleration which may be attributed to the bottom structural elasticity. Therefore two types of the maximum acceleration were derived, a maximum faired acceleration[3] (n_m) and a pure maximum acceleration (n'_m). The faired acceleration is supposed to correspond to the acceleration of the rigid body by the experiments, which compared the two models of the identical configuration and weight but with the different structural elasticity.

The results for the conical models are presented in Table 2 and Fig. 4. The theoretical values were calculated using Eqs. (14) and (15). An oscilloscope trace is shown in Fig. 3b. The agreements between the experimental and the theoretical values are very good.

Conclusion

The formulas for the maximum water impact accelerations of the spherical and conical bodies have been derived in the closed form. The experiments were carried out systematically to check the analytical results. The agreements between the experimental and the theoretical values are quite satisfactory. A further theoretical study is desirable to clarify the oscillatory phenomena of the acceleration-time history observed in the experiments.

References

[1] von Kármán, T., "The Impact on Seaplane Floats during Landing," TN 321, 1929, NACA.

[2] McGehee, J. R., Hathaway, M. E., and Vaughan, V. L., "Water-Landing Characteristics of a Reentry Capsule," MEMO 5-23-59L, June 1959, NASA.

[3] Stubbs, S. M. and Hathaway, M. E., "Effects of Bottom-Structure Flexibility on Water Landing Loads of Apollo Spacecraft Models," TN D-5108, March 1969, NASA.

[4] Lamb, H., *Hydrodynamics*, 6th ed., Cambridge Univ. Press, Cambridge, Mass., 1932.

Prediction of Terminal Variables in Homing

A. G. Rawling*
General Electric Company, King of Prussia, Pa.

Nomenclature

A = azimuth angle of velocity vector
LOS = line-of-sight connecting missile and target
M = miss distance at some specified time
R = range between missile and target along the line of sight
t = real time
V = flight velocity or speed
x,y = Cartesian coordinates
θ = angle that the relative velocity vector makes with the line of sight
σ = line of sight angle measured with respect to a fixed inertial direction in the plane

Superscripts

$(\dot{})$ = $d(\ )/dt$
$(\bar{})$ = bar denotes vector

Subscripts

0 = initial conditions existing at time $t_0 = 0$
e = conditions existing at time t_e of $\ddot{\sigma}$ first extreme
g = conditions existing at "time-to-go" t_g
I = inertial
i = conditions existing at time t_i of $\ddot{\sigma}$ first inflection point
M = missile
T = target
R = relative (as in relative velocity $\bar{V}_R$)
w = conditions existing at "time-to-pass" t_w

Introduction

THE predicted terminal behavior of passive kinematic variables such as the line of sight angle, its rate, and its acceleration (as well as the active variables range and range rate) is of major importance in rendezvous, inspection, and interception. Direct application can be made to the fields of fuzing on target and/or countermeasures, directional warhead aiming (in addition to safing, arming, and self-destruction), timely deployment of submissiles, adaptive control of onboard data processing parameters, physical homing simulators, and proper design of tracking systems and seeker gimbal mountings.

Terminal behavior is assumed herein to describe the tactical situation existing during the final closing moments of interception when the missile is unable to execute promptly any significant guidance command, as a result of hardware limitations, time lags, or inertial mass. In such a case, mission considerations may still dictate that the tracking system be able to retain the target within the sensor field of view. In addition, error comparison between measured variables and their onboard predicted values may be used to actuate devices and control ordered sequences of interrelated actions.

It is the twofold purpose of this Note to supply both qualitative and quantitative information on the terminal behavior of the kinematic variables during the interception final phase. Explicit expressions are given for the quantities as functions of time and their corresponding graphical over all behavior is shown. In addition, their predicted terminal values at the future instant of closest separation are given as functions of existing measurements taken at the time of observation.

Although all expressions given are for the case of two-dimensional planar interception, this situation is closely approximated in three dimensions by the inclined plane of interception defined by the missile and target velocity vectors in the terminal homing phase.

Kinematics

Figure 1 combines two distinct but related coordinate systems for depicting interception by a point missile and target both flying constant speed, rectilinear flight paths in the plane. Absolute Cartesian coordinates, denoted by the fixed inertial axes (x_I,y_I), are imposed on the physical situation, with both target and missile moving for $t > t_o = 0$, and the resulting action is shown above the initial LOS in Fig. 1.

For relative coordinates, with the ensuing action shown below the LOS, the target is considered fixed at its initial position, with the missile flying a path defined in direction by the relative velocity vector (and with that same speed).

Received February 27, 1970.

* Consulting Engineer, Guidance, Re-Entry and Environmental Systems Division. Member AIAA.

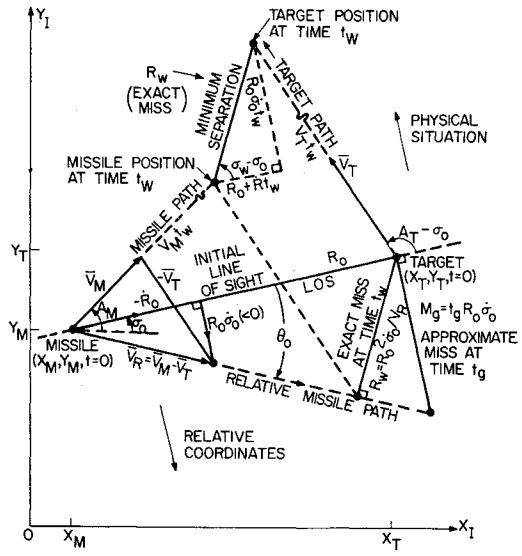

Fig. 1 Two dimensional interpretation in physical and relative coordinates.

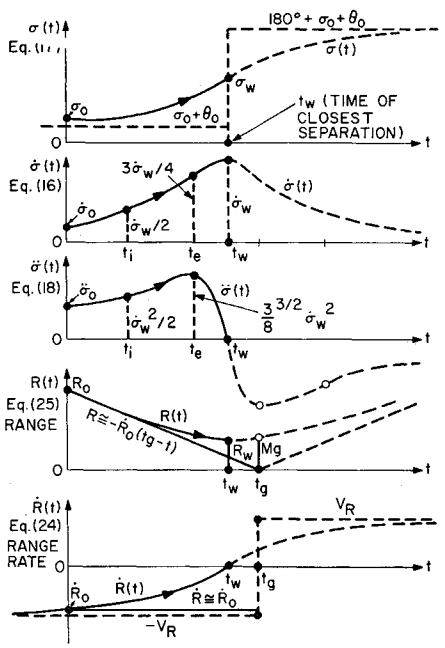

Fig. 2 Behavior of kinematic variables.

For the physical situation shown in Fig. 1 the governing nonlinear differential equations may be written[1,2]

$$\dot{R} = V_T \cos(A_T - \sigma) - V_M \cos(A_M - \sigma) \quad (1)$$

$$R\dot{\sigma} = V_T \sin(A_T - \sigma) - V_M \sin(A_M - \sigma) \quad (2)$$

where the variables are defined in the nomenclature. Appropriate initial conditions at time $t_o = 0$, which is the reference instant of observation, measurement or calculation, are

$$\begin{aligned} R(0) &\equiv R_o(>0) \qquad \sigma(0) \equiv \sigma_o \\ \dot{R}(0) &\equiv \dot{R}_o(<0) \qquad \dot{\sigma}(0) \equiv \dot{\sigma}_o \end{aligned} \quad (3)$$

Eqs. (1) and (2) may be evaluated algebraically to provide range rate and LOS angular rate, and integrated numerically with initial conditions to give the range $R(t)$ and LOS angle $\sigma(t)$, if desired.

Under the stated flight path conditions, the relative velocity vector $\bar{V}_R = \bar{V}_M - \bar{V}_T$ will be constant, with its scalar speed $|V_R|$ defined by

$$V_R^2 = V_M^2 + V_T^2 - 2V_M V_T \cos(A_T - A_M) = \dot{R}^2 + R^2\dot{\sigma}^2 \quad (4)$$

Redifferentiation of Eq. (2) and substitution leads to the differential equation for the missile acceleration perpendicular to the LOS,

$$R\ddot{\sigma} + 2\dot{R}\dot{\sigma} = 0 \quad (5)$$

useful in the following several ways.

In the case of linearization,[2] i.e., small angular deviations of the flight path from the ideal collision course (which is characterized by $\dot{\sigma} = 0$ and $\dot{R} < 0$), the remaining flight time at any instant may be approximated by either an active or passive expression for the "time-to-go," t_g

$$t_g = R_o/-\dot{R}_o = 2\dot{\sigma}_o/\ddot{\sigma}_o \quad (6)$$

The relative velocity vector $\bar{V}_R$ makes with the LOS an angle θ of the opposite algebraic sign as either $\dot{\sigma}$ or $\ddot{\sigma}$ (since Eq. (5) shows they are both positive or negative together)

$$-\tan\theta_o = R_o\dot{\sigma}_o/-\dot{R}_o = t_g\dot{\sigma}_o = 2\dot{\sigma}_o^2/\ddot{\sigma}_o \quad (7)$$

Integration of Eq. (5) with initial conditions of Eq. (3) yields the invariant relating range and LOS angular rate at any time,

$$R^2\dot{\sigma} = R_o^2\dot{\sigma}_o \quad (8)$$

Redifferentiation of Eq. (1) and substitution yields the analogous differential equation for the missile acceleration parallel to the LOS,

$$\ddot{R} - R\dot{\sigma}^2 = 0 \quad (9)$$

Integration of Eq. (9) with initial conditions leads to an expression basic for developing all the prediction equations,

$$\dot{R}^2 = R_o^2\dot{\sigma}_o[\dot{\sigma}_w - R_o^2\dot{\sigma}_o/R^2] \quad (10)$$

wherein a certain cluster of initial values is formally represented by the symbol $\dot{\sigma}_w$,

$$(\ddot{\sigma}_o^2 + 4\dot{\sigma}_o^4)/4\dot{\sigma}_o^3 \equiv \dot{\sigma}_w \quad (11)$$

whose physical significance will be identified later.

In Ref. 1, the time-to-pass t_w was derived in both an active and passive form

Table 1 Values of kinematic variables[a]

Name	Times (in order of occurrence)	Angle $\sigma(t)$, Eq. (17)	Angular rate $\dot{\sigma}(t)$, Eq. (16)	Angular accel. $\ddot{\sigma}(t)$, Eq. (18)	Range $R(t)$, Eq. (15)	Range rate $\dot{R}(t)$, Eq. (10)
1. Initial observation (quantities measured or calculated)	$t_o = 0$	σ_o	$\dot{\sigma}_o$ $[\tan\theta_o = -2\dot{\sigma}_o^2/\ddot{\sigma}_o;\ \theta_o = \sigma_w - \sigma_o \pm 90°;\ V_R = (\dot{R}_o^2 + R_o^2\dot{\sigma}_o^2)^{1/2}]$	$\ddot{\sigma}_o$	R_o	$\dot{R}_o$
2. Time of $\ddot{\sigma}$ first inflection Eq. (21)	$t_i = t_w - 1/\lvert\dot{\sigma}_w\rvert$	$\sigma_i = \sigma_w \mp 45°$ $= \pm 45° + \sigma_o + \theta_o$	$\dot{\sigma}_i = \dot{\sigma}_w/2$	$\ddot{\sigma}_i = \pm\dot{\sigma}_w^2$	$R_i = 2^{1/2}R_w$	$\dot{R}_i = -R_w\lvert\dot{\sigma}_w\rvert/2^{1/2}$ $= -V_R/2^{1/2}$
3. Time of $\dddot{\sigma}$ first extreme Eq. (20)	$t_e = t_w - 1/3^{1/2}\lvert\dot{\sigma}_w\rvert$	$\sigma_e = \sigma_w \mp 30°$ $= \pm 60° + \sigma_o + \theta_o$	$\dot{\sigma}_e = 3\dot{\sigma}_w/4$	$\ddot{\sigma}_e = \mp 3^{3/2}\dot{\sigma}_w^2/8$	$R_e = 2R_w/3^{1/2}$	$\dot{R}_e = -R_w\lvert\dot{\sigma}_w\rvert/2$ $= -V_R/2$
4. Time-to-pass (nearest approach) Eq. (12)	$t_w = \frac{2\dot{\sigma}_o\ddot{\sigma}_o}{\ddot{\sigma}_o^2 + 4\dot{\sigma}_o^4}$	$\tan(\sigma_w - \sigma_o) = \ddot{\sigma}_o/2\dot{\sigma}_o^2$ $\sigma_w = \pm 90° + \sigma_o + \theta_o$	$\dot{\sigma}_w = \frac{\ddot{\sigma}_o^2 + 4\dot{\sigma}_o^4}{4\dot{\sigma}_o^3}$	$\ddot{\sigma}_w = 0$	$R_w = \frac{2R_o\dot{\sigma}_o^2}{[\ddot{\sigma}_o^2 + 4\dot{\sigma}_o^4]^{1/2}}$ $= R_o^2\lvert\dot{\sigma}_o\rvert/V_R$	$\dot{R}_w = 0$
5. Time-to-go ($t_g > t_w$) Eq. (6)	$t_g = 2\dot{\sigma}\sigma/\ddot{\sigma}\sigma$ $= t_w + 1/t_w\dot{\sigma}_w^2$	$\sigma_g = \sigma_w - \theta_o$ $= \pm 90° - \theta_o$	$\dot{\sigma}_g = 1/\dot{\sigma}_o t_g^2$	$\ddot{\sigma}_g = -2/\dot{\sigma}_o t_g^3$	$R_g = R_o\lvert\dot{\sigma}_o\rvert t_g$ $= M_g$	$\dot{R}_g = R_o\lvert\dot{\sigma}_o\rvert$

[a] Choice of sign: upper (lower) algebraic sign implies $\dot{\sigma}_o > 0$ (<0).

$$t_w = -\dot{R}_o R_o/V_R^2 = 2\dot{\sigma}_o\ddot{\sigma}_o/(\ddot{\sigma}_o^2 + 4\dot{\sigma}_o^4) \quad (12)$$

It represents the time elapsing from $t_o = 0$ until actual minimum separation distance occurs between missile and target under the stated flight conditions. Unlike the time-to-go, t_g, t_w is valid for large angular deviations of the missile from the ideal collision course. From Eqs. (6, 7, and 12) it follows that t_w occurs before t_g,

$$t_w = t_g(-\dot{R}/V_R)^2 \equiv t_g \cos^2\theta_o \leqslant t_g \quad (13)$$

and in conjunction with Eq. (11)

$$t_w\dot{\sigma}_w = \ddot{\sigma}_o/2\dot{\sigma}_o^2 = 1/t_g\dot{\sigma}_o = -\cot\theta_o \quad (14)$$

Defining Equations

The necessary development has been completed for the prediction of LOS angle, rate, and acceleration as well as range and range rate at the instant of closest separation.

Integration of Eq. (10) with initial conditions gives the range $R(t)$ in the form

$$R^2 = R_o^2\dot{\sigma}_o[1 + \dot{\sigma}_w^2(t_w - t)^2]/\dot{\sigma}_w \quad (15)$$

Identification with Eq. (8) leads to the expression for LOS angular rate $\dot{\sigma}$,

$$\dot{\sigma}(t) = \dot{\sigma}_w/[1 + \dot{\sigma}_w^2(t_w - t)^2] \quad (16)$$

which reduces at time $t = t_w$ to $\dot{\sigma}(t_w) \equiv \dot{\sigma}_w$. Hence, Eq. (11) represents the LOS rate at t_w as predicted from the initial values at the instant of observation.

Integration of Eq. (16) with initial conditions provides a prediction expression for the LOS angle $\sigma(t)$ in the implicit form

$$\tan[\sigma(t) - \sigma_o] = \dot{\sigma}_w t/[1 + \dot{\sigma}_w^2 t_w(t_w - t)] \quad (17)$$

Differentiation of Eq. (16) leads to the desired expression for LOS angular acceleration $\ddot{\sigma}$,

$$\ddot{\sigma}(t) = 2\dot{\sigma}_w^3(t_w - t)/[1 + \dot{\sigma}_w^2(t_w - t)^2]^2 \quad (18)$$

With the aid of Eq. (16), it can be written in a useful alternate form

$$(t_w - t)\dot{\sigma}_w = \ddot{\sigma}/2\dot{\sigma}^2 \quad (19)$$

which when evaluated at $t_o = 0$ gives the interesting relation $\dot{\sigma}_w t_w\dot{\sigma}_o t_g = 1$ in agreement with Eq. (14).

The LOS acceleration $\ddot{\sigma}(t)$, as defined by Eq. (18) has a maximum and minimum (in that order, if $\dot{\sigma}_o > 0$) located symmetrically about the zero at $t = t_w$. It also possesses three inflection points, one of which is the time t_w of closest approach. By conventional successive differentiation and equating the results to zero, these critical times are found to be

$$\text{extremes:} \qquad t_e = t_w \pm 1/3^{1/2}\dot{\sigma}_w \quad (20)$$

$$\text{inflections:} \qquad t_i = t_w, \quad t_i = t_w \pm 1/\dot{\sigma}_w \quad (21)$$

The time t_e will provide the value of the first extreme of $\ddot{\sigma}$ (occurring before closest separation is reached), which is of importance in estimating the saturation constraint in the gimbal design of tracking systems.[3]

Predicted Terminal Values

Evaluation of the expressions for kinematic variables previously developed at the time t_w, of closest separation is straightforward using Eq. (12) in the case of the three passive variables (LOS angle, rate, and acceleration). Table 1 summarizes the quantity, its name, defining equation number, and evaluated expression at various times of interest, as well as t_w. Figure 2 identifies those times in the over all behavior of the kinematic variables. (Reference 4 develops curves similar to those of Fig. 2, normalized as a function of nondimensionalized time, for the case of a ground fixed radar site tracking a crossing target whose course and speed are specifiable a priori).

Evaluation of the range $R(t)$ at the time t_w predicts the exact miss distance[2]

$$R_w = 2R_o\dot{\sigma}_o^2/(\ddot{\sigma}_o^2 + 4\dot{\sigma}_o^4)^{1/2} = R_o^2|\dot{\sigma}_o|/V_R \quad (22)$$

as a function of initial observations. Note an initial range measurement R_o is required for the prediction. The linearized approximation to miss distance is predicted at time-to-go t_g, and is given[2] by

$$R_w \cong M_g = R_o|\dot{\sigma}_o|t_g \quad (23)$$

Both these miss distances are shown in Fig. 1 and 2.

The usual linearization process provides the approximations for range rate as $\dot{R}_o \cong -V_R$, a constant, and range as $R \cong -\dot{R}_o(t_g - t)$. For comparison with the exact expressions, rewrite Eq. (10) for range rate in the form

$$\dot{R}(t) = -V_R|\dot{\sigma}_w|(t_w - t)[1 + \dot{\sigma}_w^2(t_w - t)^2]^{-1/2} \quad (24)$$

and Eq. (15) for range as

$$R(t) = V_R(t_w - t)[1 + \dot{\sigma}_w^{-2}(t_w - t)^{-2}]^{1/2} \quad (25)$$

These functions, together with their linearized approximations are also shown as functions of time in Fig. 2. Note the approximation $\dot{R}_o$ for $\dot{R}$ exhibits the wrong sign before t_g is attained (after t_w has already occurred).

References

[1] Rawling, A. G., "Passive Determination of Homing Time," *AIAA Journal*, Vol. 6, No. 8, Aug. 1968, pp. 1604–1606.

[2] Rawling, A. G., "On Non-Zero Miss Distance," *Journal of Spacecraft and Rockets*, Vol. 6, No. 1, Jan. 1969, pp. 81–83.

[3] Gebhart, C., "Intercept Dynamics," *National Aerospace Electronics 1963 Proceedings*, Dayton Section Professional Group on Aerospace and Navigation Electronics, Dayton, Ohio, pp. 46–53.

[4] Chestnut, H. and Mayer, R. W., *Servomechanisms and Regulating System Design*, 1st ed., Vol. 2, Wiley, New York, 1955, pp. 44–49.

Lumped-Parameter Modeling vs Distributed-Parameter Modeling for Fluid Control Lines

G. M. SWISHER*
Wright State University, Dayton, Ohio

AND

E. O. DOEBELIN†
Ohio State University, Colombus, Ohio

THE over-all performance of a hydraulic control system is determined in part by the dynamic characteristics of the transmission lines connecting the components of the systems. Failure to account for transmission line dynamics can lead to serious errors in system design. Ezekiel and Paynter[1] derived ordinary differential equations in hyperbolic operators relating pressures and flows at two cross sections of a hydraulic line. These equations were referred to as the water-hammer equations or transfer function of the fluid lines. The literature abounds with line-dynamics information, but no investigator has applied this knowledge to the study of the interactions of line dynamics with complete control systems.

Received February 25, 1970.

* Assistant Professor of Engineering.

† Professor of Mechanical Engineering.